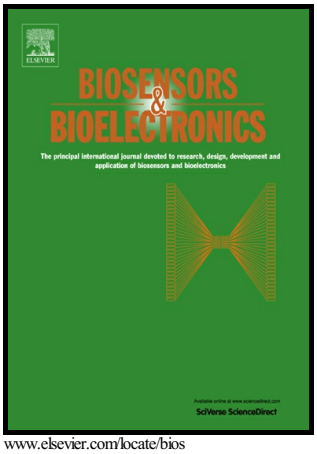

www.elsevier.com/locate/bios

DNAzyme-integrated plasmonic nanosensor for bacterial sample-to-answer detection

Fang Yu, Yun Li, Mingyu Li, Longhua Tang, Jian-Jun He

PII: S0956-5663(16)30989-7
DOI: http://dx.doi.org/10.1016/j.bios.2016.09.103
Reference: BIOS9215

To appear in: *Biosensors and Bioelectronic*

Received date: 2 August 2016
Revised date: 18 September 2016
Accepted date: 28 September 2016

Cite this article as: Fang Yu, Yun Li, Mingyu Li, Longhua Tang and Jian-Jun He, DNAzyme-integrated plasmonic nanosensor for bacterial sample-to-answe detection, *Biosensors and Bioelectronic* http://dx.doi.org/10.1016/j.bios.2016.09.103

DNAzyme-integrated plasmonic nanosensor for bacterial sample-to-answer detection

Fang Yu, Yun Li, Mingyu Li, Longhua Tang*, Jian-Jun He

State Key Laboratory of Modern Optical Instrumentation, College of Optical Science and Engineering, Zhejiang University, Hangzhou 310027, China

*Corresponding author: lhtang@zju.edu.cn

ABSTRACT

Pathogenic bacteria pose a serious threat to public safety and health, and cause significant losses in the global economy and in lives. The current golden standard, culture-based method, for bacterial detection is often costly, laborious, and time-consuming (even weeks). Thus, there is an urgent need to develop rapid, reliable and easy-to-use approaches for bacterial detection. Herein, we present a new detection strategy termed as 'DNAzyme-Integrated Plasmonic Nanosensor' (DIPNs) that can selectively detect target bacteria in a simple, inexpensive and culture-free process, which combines real-time DNAzyme-based sensor and enzyme-responsive nanoplasmonic biosensor system. The DIPNs platform takes advantage of a bacteria-specific RNA-cleaving DNAzyme probe as the molecular recognition element and enzyme-responsive plasmonic nanoparticles' localized surface plasmon resonance (LSPR) as the signal readout. Using *Escherichia coli* (*E. coli*) as a model analyte, we demonstrated that the DIPNs system can

provide the fast and low concentration (down to 50 bacteria per mL) quantification of *E. coli* even in the complex fluids (*e.g.,* milk, serum, juice) with naked eyes, which would be expected for the detection of bacterial pathogens in the simple, low-cost and on-site manner.

Keywords: Plasmonic nanosensor, bacterial pathogens, silver nanoplates, localized surface plasmon resonance, DNAzyme

1. Introduction

Rapid, sensitive and cost-effective identification of infectious agents (*e.g.*, pathogenic bacteria) are critical to prevent a potential large-scale outbreak.(Zourob, Elwary et al. 2008) However, the present golden standard, culture-based methods, for bacterial detection are costly, laborious, and time-consuming (even weeks).(Alivisatos 2004, Zhang, Geng et al. 2009, Kang, Ali et al. 2014, Tram, Kanda et al. 2014, Chen, Xianyu et al. 2015, Settu, Chen et al. 2015, Gayathri, Mayuri et al. 2016, Wang, Wang et al. 2016, Zhang, Shen et al. 2016) Recently, the state-of-the-art amplification-based molecular assays, including polymerase chain reaction (PCR)(Zhang, Shen et al. 2016) and enzyme-linked immunosorbent assays (ELISA),(Wang, Wang et al. 2016) can offer high sensitivity and in some cases high selectivity, but often require culture-enrichment steps. Additionally, being label-and instrument-dependent, these methods typically involve complicated sampling process (*e.g.*, cell lysis, extraction, separation, concentration, and signal amplification), expensive or bulky equipment and highly trained personnel, which not only result in significantly reduced testing efficiency and accuracy, but also limit their widespread utility especially in the on-site testing.(Zhang, Geng et al. 2009, Kang, Ali et al. 2014, Tram, Kanda et al. 2014, Chen, Xianyu et al. 2015)Therefore, there is an urgent demand to develop new

diagnostic strategies that are suitable for the simple-to-use, rapid and reliable detection of bacterial pathogens.

Owing to their highly tunable localized surface plasmon resonance (LSPR) properties, plasmonic nanostructures have been widely used for (bio)sensing, imaging and other nano-photonic applications.(Rosi and Mirkin 2005, Willets and Van Duyne 2007, Anker, Hall et al. 2008, Mayer and Hafner 2011, De La Rica and Stevens 2012, Rodríguez-Lorenzo, de La Rica et al. 2012, De La Rica and Stevens 2013, He, Xu et al. 2013, Peng, Xiong et al. 2014)The LSPR originates from light excited collective surface plasmon oscillations on the surface of metallic nanoparticles, which strongly depends on the metal nanoparticles' size, shape/morphology and inter-particle distance.(Mayer and Hafner 2011) In particular, such finely tunable plasmonic properties can be reflected in color change and absorption peak shift, rendering them good candidates for sensitive colorimetric (bio)sensing applications.(Peng, Xiong et al. 2014)Pioneer works have shown the advantages in using plasmonic nanoparticles (*e.g.*, silver and gold nanoparticles) for the detection and differentiation of bacteria.(Zhang, Geng et al. 2009) However, most of these nanaplasmonic biosensing methods still encounter a number of engineering and sampling challenges for bacteria detection. First, the surface physico-chemical modifications lead to nanoparticles irreversible aggregation, resulting in low detection reproducibility and accuracy.(Chen, Chung et al. 2015, Chen, Xianyu et al. 2015)Also, the existing pathogen plasmonic nanosensors are unable to directly expose to potential fields or unprocessed sample because of the nonspecific binding, thus requiring the extensive sample preparation (*e.g.*, concentration and separation).(Rosi and Mirkin 2005) Moreover, the insufficient limit of detection (LOD; typically > 1,000 colony-forming unit (cfu) per mL) would significantly limit the plasmonic nanosensor relevance for its practical applications.(Kang, Ali et

al. 2014) It is thus critical to develop new strategy to allow plasmonic nanosensors for the bacterial pathogens on-site and/or point-of-care (POC) testing.

To meet these challenges, herein, we propose the detection method termed 'DNAzyme-Integrated Plasmonic Nanosensor'(DIPNs) that can selectively detect target bacteria in a sensitive and culture-free process. The DIPNs platform combines real-time DNAzyme-based sensor and enzyme-responsive nanoplasmonic biosensor system. DNAzymes (also called deoxyribozymes, catalytic DNAs or DNA enzymes) are short synthetic oligonucleotide molecules with catalytic activity which can be isolated *in vitro* method called systematic evolution of ligands by exponential enrichment (SELEX).(Ellington and Szostak 1990, Tuerk and Gold 1990, Xia, Ye et al. 2013) Since their first discovery, DNAzymes have been functionalized for the various exceptional sensors development.(Liu and Lu 2003, Liu, Cao et al. 2009, Zhang, Geng et al. 2009, Wu, Hwang et al. 2013, Hwang, Wu et al. 2014) Herein, our used DNAzyme was designed to selectively react with the lysate to target bacteria, which has been successfully demonstrated the robustness for label-free low concentration quantification of bacteria in spiked blood.(Ali, Aguirre et al. 2011, Aguirre, Ali et al. 2013) Meanwhile, noble metal nanoparticles are intriguing nanoprobes for the biosensing applications when their LSPR shifts in response to a biomolecular recognition event.(Stewart, Anderton et al. 2008, De La Rica and Stevens 2012, Rodríguez-Lorenzo, de La Rica et al. 2012, De La Rica and Stevens 2013, Yang, Ren et al. 2015) In our proposed enzyme-responsive nanoplasmonic evolution system, silver triangular nanoplates (silver TNPs, also referred to as silver nanoprisms, silver nanotriangles) were chosen as the signal readout element, whose morphology can be evoluted from intact triangle to sphere-like nanoplate under enzymatic reaction-trigger chemical etching process, resulting in the programmablly variable LSPR properties.(He, Xu et al. 2013, Malile and

Chen 2013, Yang, Ren et al. 2015) To ensure the sample-to-answer detection of bacteria, we integrated both of sensing elements through cascaded signal amplification processes of hybridization chain reaction (HCR) and enzymatic catalysis on magnetic beads (MBs), where DNAzyme was used as recognition molecular and enzyme-responsive nanoplasmonic LSPR was used for signal readout. Using *Escherichia coli* (*E. coli*) as a model analyte, we demonstrated that the DIPNs assay system can provide fast and low concentration (down to 50 cfu per mL) quantification of *E. coli* even in complex fluids with naked eye or monitoring the LSPR shift.

2. Materials and methods

2.1 Materials

$AgNO_3$, $NaBH_4$, NaCl, polyvinylpyrrolidone (PVP, 40 kDa), Trisodiumcitrate dihydrate (Na_3CA), H_2O_2 (30% w/w) and glucose were purchased from Sigma-Aldrich. The oligonucleotides, glucose oxidase, lysozyme and serum used in this work were synthesized from Sangon Biotech. Co. Ltd. (Shanghai, China). All other chemicals were of analytical grade and obtained from Sinopharm Chemical Reagent Co. Ltd. The above reagents were uses without further purification and Milli-Q water (18 $M\Omega \cdot cm^{-1}$) was used to prepare all aqueous solutions. Milk (Mengniu skim milk) and apple juice (Minute Maid) were purchased from a local supermarket. River water was fetched from River nearby campus. The sequences of these oligonucleotides are provided in supplementary Table S1.

2.2 DIPNs for bacteria assay

Samples containing intended bacteria were incubated with bacterial lysis agent (lysozyme, 1 mg/mL) to obtain the crude cellular extraction (CCE). Then, different concentrations of bacteria CCE solution were obtained in a final volume of 10 mL reaction buffer (RB; 1 mM HEPES, pH

7.4, 150 mM NaCl, 15 mM $MgCl_2$, 0.01% tween 20). Next, MBs-DNAzyme (100 nM) were added into the diluted CCE solution in a volume of 200 μL reaction buffer. For the experiment of bacterial detection, the concentrations of *E. coli* used were 5×10^6, 5×10^5, 5×10^4, 5×10^3, 5×10^2, 50 and 0 cfu/mL. The reaction mixture was shaken at 1200 rpm at 37 ^oC for 15 min. After magnetic separation, the collected precipitate were re-dispersed and then mixed with H_1 (500 nM) and H_2 (500 nM) in Tris-Ac buffer (200 μL; pH = 6.8; 10 mM Tris, 500 mM NaAc, 0.05% Triton-100) at room temperature for 1 h. Prior to the above HCR step, both of the 50 μM of hairpin DNA H1 and H2 in buffer (10 mM Tris-Ac, 500 mM NaAc, pH = 6.8) were first heated to 95 ^oC for 5 min and then allowed to cool to room temperature in 2 h before use. After magnetic separation, avidin-GOx (10 μL,1 mg/mL) was mixed with the magnetic beads in Tris-Ac buffer (total volume: 100 μL). Next, the magnetic beads were separated and then washed three times with Tris-Ac buffer to remove free avidin-GOx. The magnetic beads were mixed with glucose (1.0 mM) in 100 μL of water for 1 h. The supernatant was mixed with the silver TNPs (100 μL, the silver TNPs were centrifuged once before use) for 20 min. Then the absorption was measured on the UV-vis spectrophotometer.

2.3 Characterization

Scanning electron microscopy (SEM) images were obtained using a Hitachi S4800 scanning electron microscope. High-resolution transmission electron microscopy (HRTEM: JEM- 2010, operated at 200 kV) and low-resolution transmission electron microscopy (TEM: H-800) were used to characterize the morphology microstructure. TEM samples were prepared by placing a drop of the final product on a carbon-coated copper grid and drying under ambient condition. The absorption and reaction kinetics were measured on the UV-vis spectrometry (Thermofisher Evolution 201). Error bars represent the standard deviations for measurements taken from 3~5

independent experiments. Fluorescence measurements were conducted at F-7000 Hitachi spectrometer. In a typical experiment, 100 μL sample was used. The fluorescence was monitored with excitation wavelength of 470 nm.

3. Results and discussion

3.1 Working principle of the DNAzyme-integrated plasmonic nanosensor (DIPNs)

The working principle of the assay is schematically illustrated in Scheme 1, which combines bacteria-specific recognition unit of DNAzyme, dual-signal amplification with cascaded DNA hybridization and enzymatic reaction processes and intrinsic sensitivity of plasmonic nanosensor. The biotinylated DNAzyme are first attached onto streptavidin-coated MBs, which can specifically respond to *E. coli* lysate. Following the addition of the target, the DNAzyme will bind with target and thereby break down the DNAzyme substrate into two pieces (Scheme 1a). Upon the target-induced cleavage and magnetic separation, the DNAzyme residual after cleavage, on the MBs, donated as DRaC-MBs, will initiate HCR process between two hairpin oligonucleotides (H1 and H2). The cascaded hybridization events will result in the formation of a long linear DNA duplex with nicked sites, and then the multiple glucose oxidase (GOx) units can be anchored on the DNA structure through the biotin-streptavidin interaction between hairpin DNA H1 and GOx (Scheme 1b). Since GOx is capable to efficiently catalyze glucose into gluconic acid and H_2O_2, the latter in turn acts as an oxidant to etch the silver TNPs into smaller spherical silver nanoparticles accompanied by a substantial blue shift of the LSPR peak (Scheme 1c), thus allowing visual detection, and realizing quantitative analysis of target bacteria.

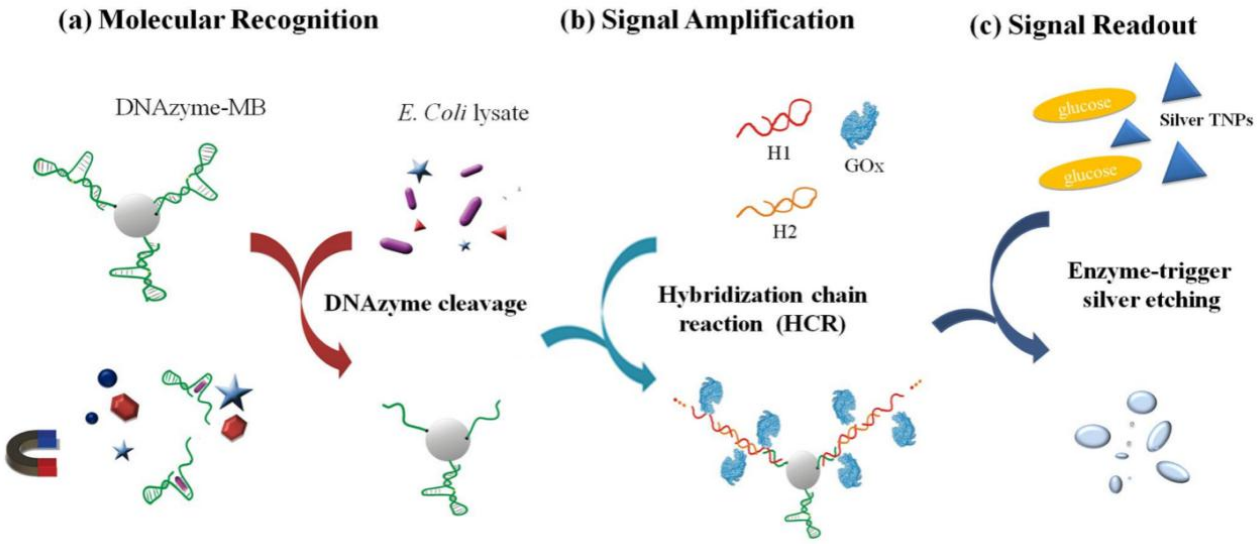

Scheme 1 DNAzyme-integrated plasmonic nanosensor (DIPNs) for *E. coli* assay.

3.2. Activity evaluation of E. coli-specific DNAzyme

The bacteria-responsive DNAzyme was first synthesized and its molecular recognition activity for the target was verified using fluorescence techniques.(Willets and Van Duyne 2007, Tram, Kanda et al. 2014) Initially, *E. coli*-specific DNAzymes are involved in our sensing strategy. The DNAzymes are generated by *in vitro* evolution of a vast random DNA library against crude extracurricular matrix (CEM) components of target bacteria. The structure of DNAzyme contains an enzyme strand and a DNA–RNA chimeric substrate strand with a single adenosine ribonucleotide (rA) in the middle as the cleavage site. Upon addition of target bacteria, DNAzyme will bind to target molecules in the produced bacterial lysate and cleave the substrate into two segments (Figure 1A). To demonstrated the DNAzyme with modification on MBs still works, a pair of fluorophore-quencher was modified in the DNAzyme, where the substrate strand was labeled with a fluorophore (Cy3) at the 5′ end and a quencher (BlackHole Quencher-2, BHQ-2) at the 3′ end. As the quenchers are in close proximity to the fluorophore, the fluorescence from Cy3 was quenched, resulting in a low background signal (Figure 1B and 1C).

Whereas, in the presence of target, a dramatically increase in fluorescence intensity was observed over time (Figure 1B). To confirm that the observed increase in fluorescence was caused by the DNAzyme recognition with bacterial lysate and not by nonspecific cleavage from other cellular components, we used the mutant enzyme sequence as a negative control (Supporting Information, Table S1). Using this inactive DNAzyme, no increase in the fluorescence was observed in the buffer or target bacteria CEM (Figure 1B), thus confirming that it was unable to cleave the native adenosine-containing substrate strand, even in the presence of target. The DNAzyme sensor maintains excellent selectivity for *E. coli* lysate over other biologically CEM (e.g., *B. subtilis*, *M. Peli*, *B. Cereus*, *B. Megaterium*, CCRF) at physiologically relevant concentrations (Figure 1C). Noted, there has been proved the pair of fluorophore-quencher modified in the DNAzyme would not affect the activity of DNAzyme. Our following work also demonstrated that the used non-dye-labeled DNAzyme still keep the selectivity to target bacterial lysate. Together, these results strongly indicate that the DNAzyme can be used to detect target *E. coli*.

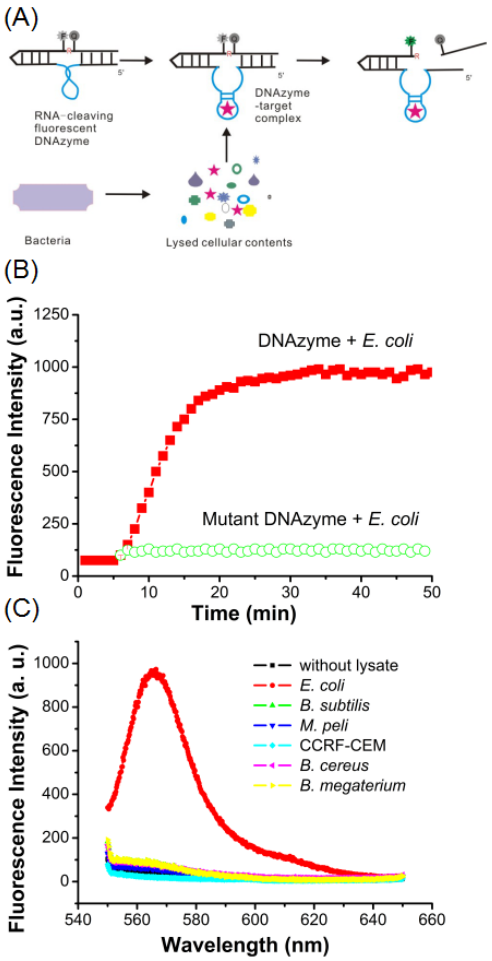

Figure 1. Real-time DNAzyme sensor selectively and rapidly detect target *E. coli* lysates. (A) Conceptual design of fluorescent DNAzymes that fluoresce upon targeting crude extracellular mixture (CEM) produced from bacterial cells. The targets produced from bacteria CEM binds to the inactive DNAzyme sequence, which undergoes a conformational change to activate the DNAzyme. The activated DNAzyme catalyzes the cleavage of the fluorogenic substrate, leading to the separation of the fluorophore (F) and the quencher (Q) to produce a high fluorescence signal. F = Cy3-dT, Q = BHQ-2-dT, R = adenosine ribonucleotide. (B) Signaling profiles of DNAzyme or mutant DNAzyme in the presence of *E. coli* CEM. (C) Fluorescence of DNAzyme in response to target bacteria with comparison to the non-target bacteria or mammalian cell human T-cell lymphoblast CCRF-CEM. Lysates from 1000 bacteria and 100 μM DNAzyme were mixed in 100 μl final volume in HEPES buffer and incubated for 20 min. Excitation wavelength: 470 nm. Emission wavelength monitored: 517 nm.

3.3 Amplified signaling the DNAzyme cleavage event by HCR process

To confirm the formation of the long nicked linear DNA structure through HCR process, fluorescence measurement was performed to reveal the relationship between the concentration of the target and the extent of the formed long DNA. SYBR Green I, a common double-stranded DNA-intercalating dye, was selected as a fluorescent indicator for the fluorescence measurement.(Zhang, Li et al. 2011) We first theoretically investigated the thermodynamic stability of the DNAzyme and experimentally demonstrated that DNAzyme residual after cleavage (DRaC) can effectively initiate HCR process (details seen in supplementary materials and Figure S1 and S2). Moreover, in the presence of the DRaC-MBs which has the identical sequence to the cleaved DNAzyme substrate, the hairpin DNA H1 and H2 mixture solution shown a hundreds-fold enhancement of fluorescence, while in the absence of the DRaC, no distinguishable fluorescence was observed (**Figure S3**). Whereas, under the same conditions of SYBR Green I (1 nM), neither the DNA solution with only DRaC or the H1 and H2 mixture with non-trigger DNA (ntDNA) showed no fluorescence was observed. These results indicated that the two hairpin DNA monomers are stable and the interaction between each other does not happen without the DRaC. Moreover, a gradually increased fluorescence intensity yielded with increasing of incubation time, suggested that more hairpin H1 and H2 were assembled into duplex DNA structure (Figure S3B inset). Noticeably, a high concentration of the DRaC resulted in the assembly of a broad range of DNA duplex structures of different lengths. This is likely due to the fact that when more trigger DNA strands are introduced, more assembly sites are formed, leaving less chance for H1 and H2 to assemble into longer structure. To minimize the assay time, we chose 20 min of HCR for the subsequent experiments.

3.4 Enzyme-triggered etching-based plasmonic nanosensor with silver TNPs

In our DIPNs system, silver TNPs were adopted as plasmonic signal indicating agents based on their unique finely tunable optical properties. Distinctive from other nanoparticles, silver TNPs contain three special sharp ‘‘corners’’ or ‘‘tips’’ that contribute significantly to their optical, electronic, and chemical properties. More importantly, the remarkably large extinction coefficient of silver TNPs makes them a sensitive indicating reagent for visual detection.(Zhang, Geng et al. 2009, Malile and Chen 2013, Yang, Ren et al. 2015) In our experiment, water-soluble silver TNPs were prepared by following an established protocol.(Zhang, Geng et al. 2009) The as-resulted silver TNPs were uniform with an edge length of 65 ± 8 nm, as transmission electron microscopy (TEM) and scanning electron microscopy (SEM) images illustrated in Figure S4A. The high yield of uniform silver nanoplates was further confirmed by the UV-vis spectrum (Figure S4B). The sharp peak around 650 nm and the weak shoulder around 420 nm can be assigned to the in-plane dipole and in-plane quadrupole plasmon resonance of silver TNPs, respectively. No sharp peak around 400 nm characteristic of spheres can be observed, confirming the high yield of silver nanoplates.

As the plasmonic visualized nanoprobes, the high stability of silver TNPs is the key for the success of the assay. In our system, we found that the dithiolated DNA molecules−functionalized silver TNPs could keep stability even in high salt and complex sample solution, preventing their etching and aggregation when exposed to sample during detection. (Figure S5-S7), and thus providing the opportunity of using these silver TNPs as the indicator in our assay.

Next, to enable visual detection with quantitative results, we proposed to convert the target recognition event into a cascaded chemical etching process and colorimetric readout. As previously illustrated, H_2O_2 can be used as an effective etchant to dissolve the metallic silver at very low concentration and induced an apparent LSPR peak shift. To evolve this concept of

tailoring LSPR by *in situ* chemical etching of silver, we used the enzyme GOx to control silver nanostructures, which generates H_2O_2 that induces chemical etching process around silver nanoparticles. The underlying chemistry involved is based on dissolving Ag from the silver TNPs using the H_2O_2, which was generated *in situ* from the surface-confined enzymatic oxidation of glucose in the presence of oxygen.(He, Xu et al. 2013, Xia, Ye et al. 2013)The reactions can be described by equations 1 and 2:

$$\text{D-glucose} + O_2 + H_2O \xrightarrow{\text{GOx}} \text{D-gluconic acid} + H_2O_2 \qquad (1)$$

$$\text{metallic silver} + H_2O_2 \xrightarrow{\text{etching}} Ag^+ + H_2O \qquad (2)$$

The etching process was inspected using UV-vis spectrometry. As shown in Figure S8, when GOx and glucose coexisted in the solution, a gradually blue shift of the SPR peak was observed. As confirmed by TEM and SEM imaging (Figure S6C, D in SI), silver anisotropic nanostructures were evolved from intact triangle to spherical nanoplate in the presence of H_2O_2, which is consistent with the fact that the extent of dipole plasmon resonance shift of the silver nanoparticles is related to the aspect ratios of the particles.(Xia, Ye et al. 2013, Yang, Yu et al. 2014, Yang, Ren et al. 2015) It was found that the etching process is GOx concentration dependent and the higher GOx concentrations produced larger blue shifts of the LSPR peak. These results pave the way for the development of a highly sensitive assay.

To establish our DIPNs sensing method, we studied the time-dependent chemical etching kinetics of silver TNPs by *E. coli* lysate-specific recognition event. Experimentally, the target *E. coli* lysate cleaved DNAzyme to release the substrate DRaC, which can trigger HCR process and then anchor multiple GOx for subsequent etching silver TNPs. Figure 2shows the typical evolution of the UV−Vis spectra of the DNA-capped silver TNPs during the etching process. The etching process induced an apparent absorption peak shift of silver TNPs from 650 nm to 530 nm with a corresponding dramatic color changes, due to the shape change of the silver TNPs

with the advance of the etching process. Thus, our assay can be used to determine target by monitoring the LSPR peak shift of silver TNPs and the correspondence color change.

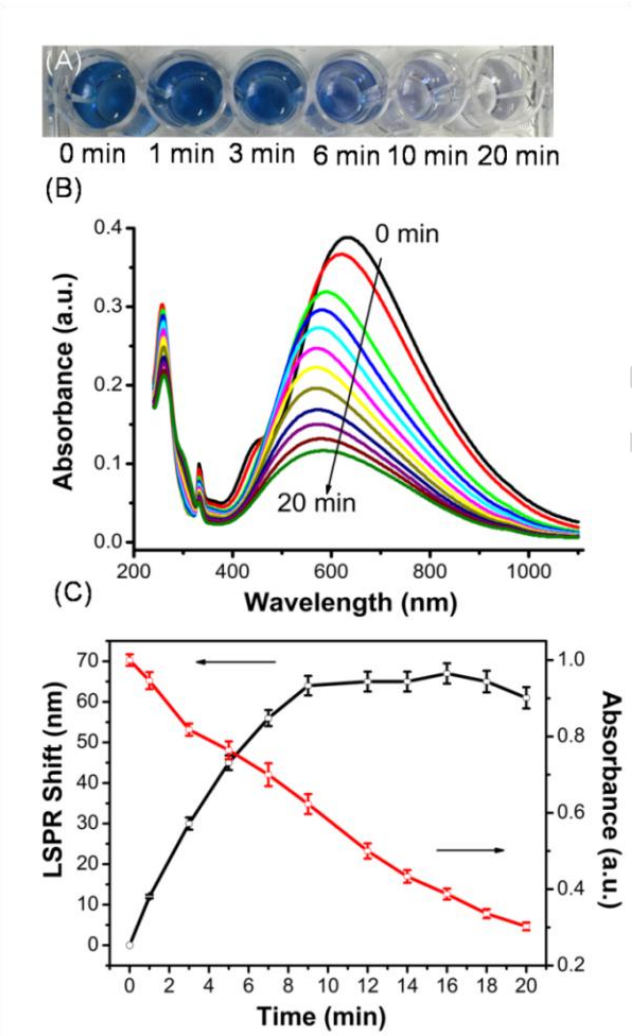

Figure 2. (A) The photograph and (B) time-dependent LSPR absorption spectra of the silver TNPs upon incubating with GOx and glucose (0, 1, 3, 5, 7, 9, 12, 14, 16, 18, 20 min). (C). The plots of LSPR peak shift (left) and absorption intensity change (right) of the silver TNPs over time in the presence of GOx and glucose. The error bars correspond to the standard deviation of fluorescence measurements across 3~5 repetitive experiments. GOx concentration: 1 μg/mL; Glucose concentration: 1 mM.

3.5 Performance of DIPNs for E. coli

After system optimization (details please see Figure S9 and Figure S10 in the SI), the DIPNs method was applied to quantify the concentration of *E. coli*. Target *E. coli* concentrations of 0 ~ 5×10^6 cfu mL^{-1}were tested with three measurements each in parallel. As shown in Figure 3A, samples containing *E. coli* were able to produce colorimetric signals, confirming that the silver TNPs-based nanosensor system could respond to bacteria *E. coli* to trigger H_2O_2 generation for colorimetric readout. Moreover, the color signal was proportional to the concentration of target, establishing the quantitative detection capability of the DIPNs assay platform. Noted, by prolonging the etching time, we could improve the detection sensitivity with the naked eyes. For instance, if silver etching time prolong to 60 min from 20 min used in Figure 3A, the concentration of 50 bacteria per ml could be easily differentiated with naked eyes .To concisely quantify the amounts of target, we further measured the LSPR change of the nanosensor system. Figure 3B shows the LSPR absorption spectra of silver TNPs solution when the silver TNPs were exposed to the *E. coli* solutions with different concentrations. Figure 3C shows the plot of LSPR peak shift of silver TNPs obtained at the etching time of 20 min against the analyte *E. coli* concentration. It shows a quasi-linear correlation in the concentration ranging from 50 cfu mL^{-1} and 2×10^3 cfu mL^{-1}. A detection limit of ~20 cfu mL^{-1} *E. coli* was observed based on 3σ/slope, where σ was the standard deviation of blank samples. Therefore, the DIPNs is one of the most sensitive culture-free *E. coli* sensor systems, which is 1~100 fold more sensitive than the previous colorimetric detection.(Zhang, Geng et al. 2009, Ali, Aguirre et al. 2011, Aguirre, Ali et al. 2013, Zhang, Shen et al. 2016) To further extend DIPNs in the field as POC testing, we can simplify the testing procedures by preparation of the analytical kit. In our future work, to further simplify the multistep operation procedure, which may limit the DIPNs for application in the

field, we will consider to prepare the analytical kits, which is expected to ensure sensing reproducibility and be better suited for field application..

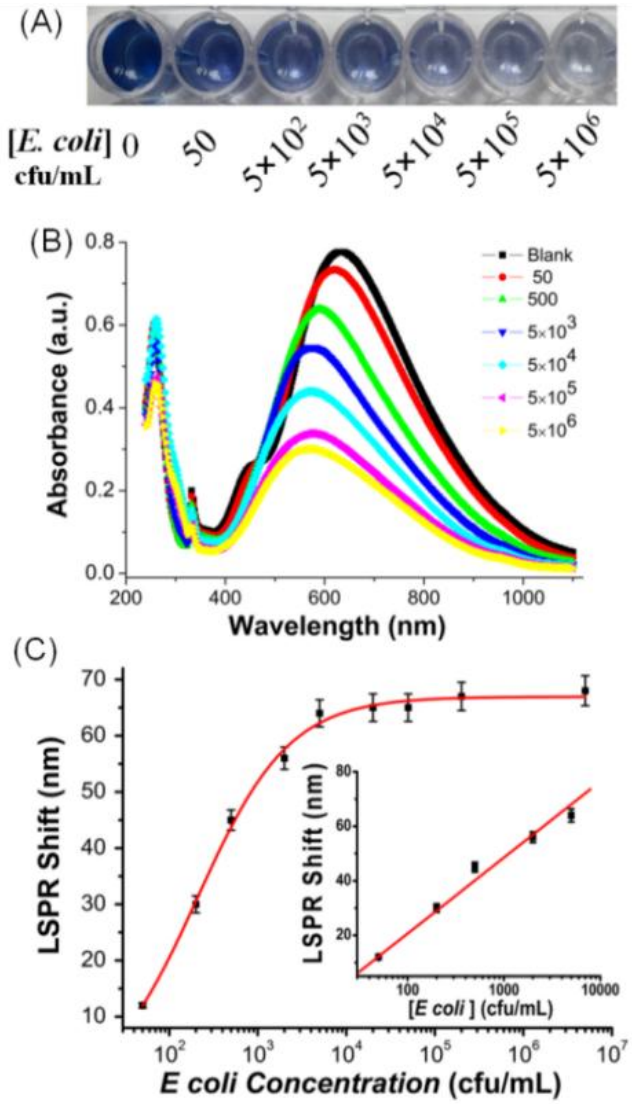

Figure 3. (A) The photographs and (B) UV-vis spectra of silver TNPs in the DIPNs assay with different concentrations of target *E. coli*. (C) The corresponding calibration curve of target concentrations vs. LSPR peak shift. The inset shows a linear plot of SPR peak shift*versus* concentrations of *E. coli*. Mean values and standard deviations were obtained from three independent experiments.

Next, to demonstrate the reliability of the DIPNs system, control and recovery experiments were studied using other bacterial lysates or matrices (Figure 4). These control groups exhibited minimal LSPR peaks shift and color change, which is close to the non-target background (Figure

4A). As for the recovery experiments in complex samples, we first spiked *E. coli* to the river water, apple juice, silk milk and goat serum, respectively, and then analyzed concentrations using the proposed method (Figure 4B). It was found that the recoveries ranged from 95.8% to104.9%, indicating that our DIPNs assay has a great selectivity and anti-interference capability even in complex media and may therefore find practical use for analysis of *E. coli* in real samples.

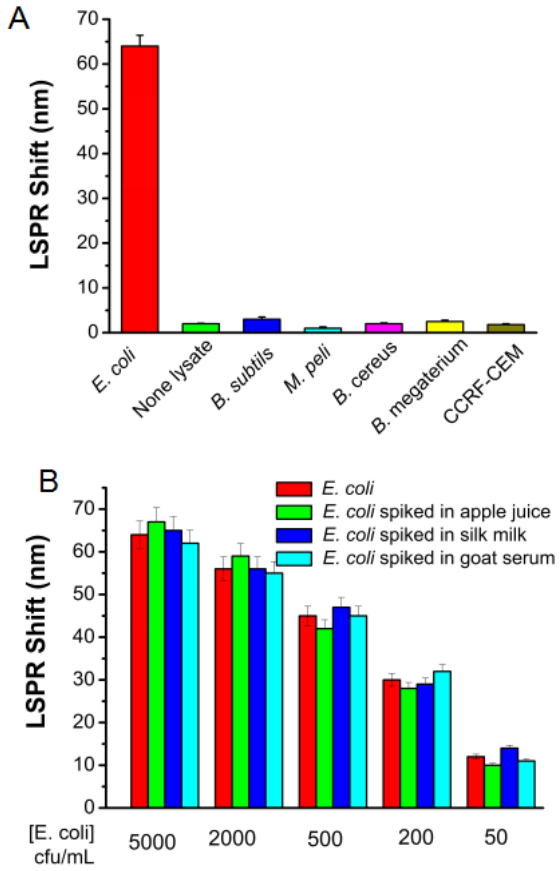

Figure 4. LSPR peak shift of the silver TNPs in our DIPNs assay towards (A) the non-target bacteria or mammalian cell human T-cell lymphoblast CCRF-CEM and (B) *E. coli* spiked in the other matrices (river water, apple juice, silk milk and goat serum). The bacteria concentrations were 5000, 2000, 500, 200 and 50 cfu mL^{-1} in samples.

Conclusions

In summary, we have demonstrated a robust sample-to-answer assay platform of DIPNs for *E. coli* that integrated both of sensing elements through cascaded signal amplification processes of hybridization chain reaction and enzymatic catalysis on magnetic beads, where DNAzyme was used as recognition molecular and enzyme-responsive nanoplasmonic LSPR as signal readout. This sensing system takes advantage of the molecular recognition unit of bacteria-specific RNA-cleaving DNAzyme and the intrinsic sensitivity of plasmonic nanosensor. Using *E. coli* as a model, we demonstrated that the assay system could be used to detect less than 50 cfu mL^{-1} of bacteria with naked eye or by monitoring the LSPR change in 2-3 hours. Noted, the DIPNs system can be further improve the sensitivity by prolonging the reaction time.The sensing performance is not only comparable to the most sensitive methods reported to date, but also can be achieved without the requirement of specialized equipment. Although an *E. coli*-sensing DNAzyme was used in the current study, the sensor design can be easily extended to any RNA-cleaving DNAzyme or aptazyme for the detection of other molecules. Moreover, with the features of fast detection and high sensitivity at the low concentration of the target bacteria, the DIPNs platform can be further developed into lab-on-a-chip devices for other biosensing applications.

Acknowledgement

This work was financially supported by National Natural Science Foundation of China (Nos.61405176 and 61535010), Natural Sciences Fund of Zhejiang Province (Nos. LY14B050004 and LY16F050001) and the Fundamental Research Funds for the Central Universities (No. 2016QNA5001) and the National High-Tech Research and Development Program of China (No.2014AA06A504).

Supporting Information Available.

REFERENCES

Aguirre, S. D., M. M. Ali, B. J. Salena and Y. Li, 2013, Biomolecules 3(3), 563-577.
Ali, M. M., S. D. Aguirre, H. Lazim and Y. Li, 2011, Angewandte Chemie International Edition 50(16), 3751-3754.
Alivisatos, P., 2004, Nature Biotechnology 22(1), 47-52.
Anker, J. N., W. P. Hall, O. Lyandres, N. C. Shah, J. Zhao and R. P. Van Duyne, 2008, Nature Materials 7(6), 442-453.
Chen, P., M. T. Chung, W. McHugh, R. Nidetz, Y. Li, J. Fu, T. T. Cornell, T. P. Shanley and K. Kurabayashi, 2015, ACS Nano 9(4), 4173-4181.
Chen, Y., Y. Xianyu, Y. Wang, X. Zhang, R. Cha, J. Sun and X. Jiang, 2015, ACS Nano 9(3), 3184-3191.
De La Rica, R. and M. M. Stevens, 2012, Nature Nanotechnology 7(12), 821-824.
De La Rica, R. and M. M. Stevens, 2013, Nature Protocols 8(9), 1759-1764.
Ellington, A. D. and J. W. Szostak, 1990, Nature 346(6287), 818-822.
Gayathri, C. H., P. Mayuri, K. Sankaran and A. S. Kumar, 2016, Biosensors and Bioelectronics 82, 71-77.
He, H., X. Xu, H. Wu, Y. Zhai and Y. Jin, 2013, Analytical Chemistry 85(9), 4546-4553.
Hwang, K., P. Wu, T. Kim, L. Lei, S. Tian, Y. Wang and Y. Lu, 2014, Angewandte Chemie International Edition 53(50), 13798-13802.
Kang, D.-K., M. M. Ali, K. Zhang, S. S. Huang, E. Peterson, M. A. Digman, E. Gratton and W. Zhao, 2014, Nat Commun., 5(5): 5427-5427.
Liu, J., Z. Cao and Y. Lu, 2009, Chemical reviews 109(5), 1948-1998.
Liu, J. and Y. Lu, 2003, Journal of the American Chemical Society 125(22), 6642-6643.
Malile, B. and J. I. Chen, 2013, Journal of the American Chemical Society 135(43), 16042-16045.
Mayer, K. M. and J. H. Hafner, 2011, Chemical Reviews 111(6), 3828-3857.
Peng, Y., B. Xiong, L. Peng, H. Li, Y. He and E. S. Yeung, 2014, Analytical Chemistry 87(1), 200-215.
Rodríguez-Lorenzo, L., R. de La Rica, R. A. Álvarez-Puebla, L. M. Liz-Marzán and M. M. Stevens, 2012, Nature Materials 11(7), 604-607.
Rosi, N. L. and C. A. Mirkin, 2005, Chemical Reviews 105(4), 1547-1562.
Settu, K., C.-J. Chen, J.-T. Liu, C.-L. Chen and J.-Z. Tsai, 2015, Biosensors and Bioelectronics 66, 244-250.
Stewart, M. E., C. R. Anderton, L. B. Thompson, J. Maria, S. K. Gray, J. A. Rogers and R. G. Nuzzo, 2008, Chemical Reviews 108(2), 494-521.
Tram, K., P. Kanda, B. J. Salena, S. Huan and Y. Li, 2014, Angewandte Chemie International Edition 53(47), 12799-12802.
Tuerk, C. and L. Gold, 1990, Science 249(4968), 505-510.
Wang, N., Y. Wang, T. Guo, T. Yang, M. Chen and J. Wang, 2016, Biosensors and Bioelectronics 85, 68-75.
Willets, K. A. and R. P. Van Duyne, 2007, Annu. Rev. Phys. Chem. 58, 267-297.

Wu, P., K. Hwang, T. Lan and Y. Lu, 2013, Journal of the American Chemical Society 135(14), 5254-5257.
Xia, Y., J. Ye, K. Tan, J. Wang and G. Yang, 2013, Analytical Chemistry 85(13), 6241-6247.
Yang, X., Y. Ren and Z. Gao, 2015, Chemistry-A European Journal 21(3), 988-992.
Yang, X., Y. Yu and Z. Gao, 2014, ACS Nano 8(5), 4902-4907.
Zhang, Q., N. Li, J. Goebl, Z. Lu and Y. Yin, 2011, Journal of the American Chemical Society 133(46), 18931-18939.
Zhang, X., P. Geng, H. Liu, Y. Teng, Y. Liu, Q. Wang, W. Zhang, L. Jin and L. Jiang, 2009, Biosensors and Bioelectronics 24(7), 2155-2159.
Zhang, X., J. Shen, H. Ma, Y. Jiang, C. Huang, E. Han, B. Yao and Y. He, 2016, Biosensors and Bioelectronics 80, 666-673.
Zourob, M., S. Elwary and A. Turner, 2008, Springer, New York.

Highlight

- A new DNAzyme-integrated plasmonic nanosensor is first developed with real-time DNAzyme and enzyme-responsive nanoplasmonic sensors.
- A new dual-signal amplification strategy of cascaded DNA hybridization and enzymatic reaction processes is proposed to achieve an ultrahigh sensitivity
- 3. A fast and low concentration (< 50 cfu/ml) quantification of *E. coli is realized* even in the complex fluids (e.g., milk, serum, juice) with naked eyes.